



A radiographic study of dorsovolar wrist axes and a database of angular measurements on axial computed tomography images

Atilla Arık, MD¹, Mustafa Yasin Hatipoğlu, MD², Burç Özcanıyüz, MD³, Mustafa Bulut, MD³,
Firat Seyfettinoğlu, MD³

¹Department of Orthopedics and Traumatology, Division of Hand Surgery, Mersin City Training and Research Hospital, Mersin, Türkiye

²Department of Orthopedics and Traumatology, Division of Hand Surgery, Adana City Training and Research Hospital, Adana, Türkiye

³Department of Orthopedics and Traumatology, Adana City Training and Research Hospital, Adana, Türkiye

The wrist is composed of numerous bones and complex joints with varying morphology and different axial orientation. The most of variations can be identified via X-ray and their respective sequences of the conventional computed tomography (CT).^[1] Since an axial CT scan accurately delineates the cross-sectional anatomy of the distal radius and carpal region, it is also useful for identifying principal reference axes, which are critical in analyzing rotational anatomy. The axial plane of the CT scan is also essential to investigate the associations between certain clinical conditions and rotational/torsional malalignments in the other skeletal regions.^[2,3]

Received: October 04, 2022

Accepted: November 22, 2022

Published online: December 27, 2022

Correspondence: Atilla Arık, MD, Mersin Şehir Eğitim ve Araştırma Hastanesi, Ortopedi ve Travmatoloji Kliniği, El Cerrahisi Bölümü, 33240 Toroslar, Mersin, Türkiye.

E-mail: atillaarik@yahoo.com

Doi: 10.52312/jdrs.2023.872

Citation: Arık A, Hatipoğlu MY, Özcanıyüz B, Bulut M, Seyfettinoğlu F. A radiographic study of dorsovolar wrist axes and a database of angular measurements on axial computed tomography images. Jt Dis Relat Surg 2023;34(1):176-182. doi: 10.52312/jdrs.2023.872

©2023 All right reserved by the Turkish Joint Diseases Foundation

This is an open access article under the terms of the Creative Commons Attribution-NonCommercial License, which permits use, distribution and reproduction in any medium, provided the original work is properly cited and is not used for commercial purposes (<http://creativecommons.org/licenses/by-nc/4.0/>).

ABSTRACT

Objectives: This study aims to identify the most accurate dorsovolar principal axis of the distal radius and carpus identified on axial computed tomography (CT) sections and to establish normative data for angular measurements among these axes.

Patients and methods: Between December 2019 and December 2021, normal axial CT images of wrists of a total of 42 individuals (25 males, 17 females; mean age: 31±8.4 years; range, 18 to 45 years) were retrospectively analyzed. Eight axes were identified on axial CT images: four distal radial axes (the volar cortical, medial cortical, central, and sigmoid notch axes) and four carpal axes (the scapholunate, lunotriquetral, capitolunate, and pisotrapezial axes). Twenty-two angular parameters were measured with reference to four principal axes (the volar cortical, medial cortical, central, and pisotrapezial axes).

Results: The mean sigmoid notch rotation (version) angles relative to the four principal axes were 8±5° (range, -2° to 18°), 6±5° (range, -2° to 13°), 1±5° (range, -8° to 14°), and 4±4° (range, -3° to 15°), respectively. The mean scapholunate rotation angles were -13±5° (range, -27° to -6°), -15±6° (range, -29° to -8°), -21±5° (range, -30° to -11°), and -8±5° (range, -28° to -6°), respectively. Among four principal axes, the volar cortical and medial cortical axes were nearly collinear with both of relatively fixed carpal axes. The four principal axes showed angular differences between 2° and 8° with each other. There was no significant difference between men and women for all measurements.

Conclusion: The axial CT sections can be used to describe the various angulations between the normal wrist axes such as the sigmoid notch and scapholunate joint rotation axes. Despite slight differences among the four principal axes, the volar cortical and medial cortical axes are more consistent with the relatively fixed carpal axes.

Keywords: Angle measurement, axis, carpal, computed tomography, distal radius, scapholunate, sigmoid notch.

The principal axes of the wrist on axial CT sections are used as a reference in the anatomical, kinematic, and clinical studies in patients with different conditions such as distal radius malunion,

distal radioulnar joint (DRUJ) instability, and scapholunate ligament injury.^[1,4-7] However, available data are problematic due to the different landmarks and principal axes preferred for reference. Several different anatomical locations have been used as a principal axis of the distal radius in the past; the central (mediolateral radiocarpal joint) axis, volar cortical axis (at distal metaphyseal level), and sigmoid notch axis.^[5,8,9] Moreover, a comparative analysis of these axes was performed only in one study partly,^[9] to the best of our knowledge.

In the present study, we aimed to identify various dorsovolar wrist axes for accurate measurements, quantify the various angular parameters between these axes, investigate the most consistent one among the four principal axes, and provide normative data for rotational angles of the DRUJ and scapholunate joint.

PATIENTS AND METHODS

This single-center, retrospective, cross-sectional study was conducted at Adana City Training and Research Hospital, Department of Orthopedics and Traumatology between December 2019 and December 2021. Normal axial CT images of the wrist stored in the hospital picture archiving and communication system (PACS) were analyzed. The criteria for inclusion of the images were as follows: patient age 18 to 45 years, images taken to evaluate the wrists due to a simple fall, a suspicion of occult carpal fracture around the wrist, and presence of a follow-up examination or radiology reporting note indicating the absence of any osseous pathology. The neutral position of the wrist was defined as the dorsal part of the middle metacarpal being aligned with the dorsal part of the radius.

All images were acquired on a 128-row multidetector CT scanner (Ingenuity Core 128; Philips Medical Systems Inc., Cleveland, OH, USA). The scan parameters were as follows: tube setting 120 kV and 30 mA; gantry rotation time 0.4 sec; field of view 150 mm; scan time 8 sec; radiation dose 420 mGy-cm. The scanned segment covered the area from 5 cm proximal of the radiocarpal joint to the base of the metacarpals. The slice thickness was set at 1.4 mm and a section interval of 0.625 mm, and the table speed was set at 1 mm/sec. All CT images were made in the standard positioning of our hospital with the patient in a prone position, their shoulder overhead in maximum abduction, the elbow in full extension, forearm in pronation, and wrist and palm in contact with the gantry. The forearm and hand were stabilized by supporting pillows and Velcro

straps to keep them at the center of the gantry and in the neutral flexion and deviation. The template was aligned with the longitudinal axis of the distal third of the ulna.

Two cases were excluded due to noticeable deformities related to the previous fractures, two for radiographic findings indicating osteoarthritis of the radiocarpal joint and DRUJ, and four were excluded due to insufficient wrist position (such as wrist flexed or extended) and suboptimal image quality (exams degraded by artifact or motion) of the CT images. The measurements were performed in the remaining 42 individuals (25 males, 17 females; mean age: 31±SD years; range, 18 to 45 years). The left-to-right ratio was 22:20.

Axes and angular measurements

Determining the radial axis (x, y, and z) is of utmost importance for reference in kinematic and anatomical studies. An anatomical and right-handed coordinate system was used for all wrists for consistent nomenclature.^[10] The z-axis represents the proximal to distal direction, the x-axis radio-ulnar, and the y-axis dorsal-to-volar. In this study, we used only x and y-axes on axial sections.

Eight axes were identified on axial CT images; four of them were distal radial axes (the volar cortical, medial cortical, central, and sigmoid notch axes) and four were carpal axes (the scapholunate, lunotriquetral, capitohamate, and pisotrapezial axis) (Table I). The volar cortical axis of the distal radius was the perpendicular to the line along the volar flat surface of the radius at the level of 15 mm proximal to the lunate facet.^[9] The medial cortical axis was the line along the medial surface of the distal radius at the level of immediately proximal to the sigmoid notch. The central axis was the perpendicular to the line connecting the styloid tip and the midpoint between the volar and dorsal margins of the sigmoid notch at the radiocarpal joint level.^[11] The sigmoid notch axis was a line connecting the volar and dorsal rims of the sigmoid notch.^[12] The scapholunate joint axis was the line passing through the midportion of the joint from dorsal to volar direction.^[13] The lunotriquetral joint axis was the line passing through the midportion of the joint from dorsal to volar direction. The capitohamate joint axis was the line passing through the proximal portion of the joint from dorsal to volar direction. The pisotrapezial axis was the perpendicular to the line connecting the most volar prominences of the pisiform and trapezium. The pisotrapezial axis is novel for this study and represents the two subcutaneous bony prominences

TABLE I Axes used in this study		
Region	Axes	Description
Distal radius	Volar cortical*	Distal radius volar cortical y-axis*
	Medial cortical*	Distal radius medial cortical axis*
	Central*	Radiocarpal joint mediolateral y-axis*
	Sigmoid notch	Sigmoid notch version axis
Carpal	Scapholunate	Scapholunate joint dorsovolar axis
	Lunotriquetral	Lunotriquetral joint dorsovolar axis
	Capitohamate	Capitohamate joint dorsovolar axis
	Pisotriquetral*	*Pisotriquetral subcutaneous y-axis

* The principal reference axes for angular measurements.

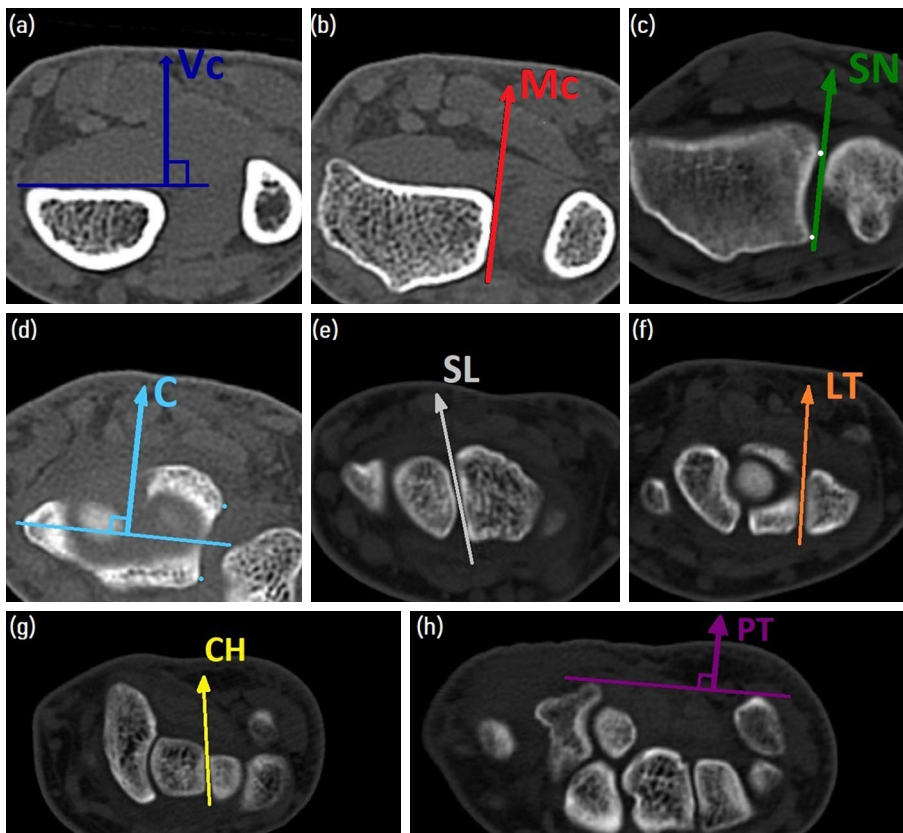


FIGURE 1. Representation of each axis on axial computed tomography images from proximal to distal. (a) Volar cortical axis (at the level of 15 mm proximal to the lunate facet); (b) Medial cortical axis (at immediately proximal to the sigmoid notch); (c) Sigmoid notch axis (at the middle level of the DRUJ); (d) Central axis; (e) Scapholunate axis; (f) Lunotriquetral axis; (g) Capitohamate axis; (h) Pisotrapezial axis (please see text and Table I for details).
 Vc: Volar cortical; Mc: Medial cortical; SN: Sigmoid notch axis; C: Central; SL: Scapholunate; LT: Lunotriquetral; CH: Capitohamate; PT: Pisotrapezial.

contacted to the table/cassette, while positioning of the wrist for posteroanterior X-ray. The medial cortical axis was also used for the first time in this study, to the best of our knowledge. Various axes

used in angular measurements are demonstrated in Figure 1. The four of these axes (the volar cortical, medial cortical, central, and pisotrapezial axes) were identified as the principal axes. Twenty-two angular

parameters were measured by referencing these four principal axes.

Before the measurements, each of the eight axes were marked on their respective axial images (Figure 1). Then, 22 angular parameters were measured by using these axes in each of 42 wrists. Angle direction was always set toward the volar side. The measured angle was defined as positive (+) if it was on the ulnar side with respect to the principal axis, and negative (-) if it was on the radial side. The first measurement group included four separate measurements of the sigmoid notch version angle with respect to the four principal axes (three distal radial and one carpal axes). The second group comprised four separate measurements of the scapholunate joint rotational angle with respect to each four principal axes. The third group was created to establish normative values of the angular differences among the four principal

axes. The fourth group was formed to determine the most consistent principal axis by referencing the two carpal axes, which are considered to be the relatively fixed unit of the carpus (Table I).^[6,14] The criterion for the most consistent radiocarpal relationship was fulfilled, when the pair of axes to be measured were nearly collinear (the angle between -5° and $+5^\circ$). All measurements were performed using the digital measurement tools of the MicroDicom viewer™ version 4.0.0 software (MicroDicom Ltd., Sofia, Bulgaria).

Measurements were performed in a random order by two independent observers who were blinded to both patients' and clinical characteristics. One was a fellowship-trained hand surgeon and the other was a fourth-year resident in orthopedic surgery. Each reviewer made a single measurement. The mean of both measurements taken for each parameter was recorded as the baseline value.

TABLE II
Descriptive data of various parameters

Angles between axes	Mean±SD	Range	95% CI	Women (n=17)	Men (n=25)
Volar cortical/sigmoid notch	8.2°±5	-1.9 to 18.4	6.5 to 10.2	7.8°±7	8.5°±4
Medial cortical/sigmoid notch	6.0±4	-2.0 to 13.1	3.8 to 8.2	6.4±5	5.8±4
Central/sigmoid notch	1.0°±5	-7.9 to 13.7	-0.7 to 2.6	-0.2°±5	1.7°±5
Pisotrapezial/sigmoid notch	3.9°±4	-3.4 to 15.2	2.4 to 5.3	4.0°±6	3.8°±3
Volar cortical/scapholunate	-13.2°±5	-27.4 to -5.7	-15.0 to -11.3	-12.1°±5	-13.8°±6
Medial cortical/scapholunate	-15.1±6	-28.5 to -8.0	-18.8 to -14.2	-14.2±4	-15.8±6
Central joint/scapholunate	-20.6°±5	-29.5 to -10.7	-22.2 to -19.0	-20.5°±5	-20.6°±5
Pisotrapezial/scapholunate	-17.7°±5	-28.2 to -5.9	-19.4 to -16.0	-16.4°±6	-18.6°±5
Volar cortical/medial cortical	1.9±5	-5.5 to 9.6	-0.5 to 4.1	2.6±4	1.7±5
Medial cortical/pisotrapezial	2.3±5	-4.6 to 12.8	-0.4 to 4.6	2.9±6	1.6±5
Pisotrapezial/central	2.9°±5	-9.4 to 15.9	1.2 to 4.6	4.1°±5	2.1°±5
Medial cortical/central joint	5.7±5	-8.7 to 13.9	1.9 to 7.3	6.0±6	4.9±5
Volar cortical/pisotrapezial	4.6°±5	-4.2 to 14.2	3.0 to 6.1	4.3°±6	4.7°±4
Volar cortical/central joint	8.1°±5	-1.4 to 19.1	6.5 to 9.6	8.9°±6	7.6°±4
Volar cortical/lunotriquetral	2.9°±4	-7.1 to 11.7	1.4 to 4.4	3.6°±5	2.4°±4
Volar cortical/capitohamate	-1.0°±6	-13.6 to 7.8	-3.0 to 1.0	-0.9°±6	-1.1°±6
Medial cortical/lunotriquetral	0.8±7	-13.7 to 13.8	-4.0 to 4.2	1.6±6	0.2±7
Medial cortical/capitohamate	-3.4±6	-12.8 to 5.7	-6.2 to -1.7	-3.4±5	-3.5±6
Central joint/lunotriquetral	-4.6°±4	-14.0 to 5.6	-6.1 to -3.0	-4.8°±5	-4.4°±5
Central joint/capitohamate	-8.4°±8	-29.2 to 7.0	-11.1 to -5.8	-9.3°±9	-7.9°±6
Pisotrapezial/lunotriquetral	-1.7°±4	-10.4 to 5.9	-3.1 to -0.2	-0.7°±5	-2.3°±4
Pisotrapezial/capitohamate	-5.6°±6	-18.6 to 11.7	-7.7 to -3.5	-5.1°±8	-5.9°±5

SD: Standard deviation; CI: Confidence interval.

Statistical analysis

Statistical analysis was performed using the IBM SPSS for Windows version 20.0 software (IBM Corp., Armonk, NY, USA). Descriptive data were expressed in mean \pm standard deviation (SD), median (min-max) or number and frequency, where applicable. The Shapiro-Wilk test was used to analyze whether each group was normally distributed. Interobserver reliability was examined using the intraclass correlation coefficient with 95% confidence interval (CI). Unpaired samples t-test (for normally distributed data) and the Mann-Whitney U test (for non-normally distributed data) were used to compare values of each parameter between male and female groups. A *p* value of <0.05 was considered statistically significant.

RESULTS

Normal values and ranges for the sigmoid notch version angle and scapholunate joint rotation angle formed relative to the four principal axes are demonstrated in Table II. The mean sigmoid notch

formed a retroverted angle with a mean of 8° with the volar cortical axis, 6° with the medial cortical axis, 1° with the central axis, and 4° with the pisotrapezial axis. Only one female had an anteverted sigmoid notch angle with -2° relative to the volar cortical axis. The mean sigmoid notch axis was found to be nearly collinear to the central axis of the radius by 1° . The scapholunate joint formed an externally rotated angle with a mean of -13° with the volar cortical axis, -15° with the medial cortical axis, -21° with the central axis, and -18° with the pisotrapezial axis (Table II).

Orientations of the four principal axes were ordered from radial to ulnar as follows: the volar cortical, medial cortical, pisotrapezial and central axes, with a mean of 2° , 3° , and 3° angular difference between them, respectively. In total, there was a mean of 8° difference between the volar cortical axis (the most radial) and the central axis (the most ulnar) (Figure 2). Both volar and medial cortical axes were the most consistent principal axes, being nearly collinear (between -5° and 5°) with the relatively fixed unit of the carpus (lunotriquetral and capitolunate joints) (Table II). Sex difference was not significant in any of the 28 measurements (Table II). Interobserver reliability was excellent for all measurements, ranging from 0.78 to 0.98.

DISCUSSION

The principal axes of the wrist on axial CT sections are used as a reference in studies for following conditions: the distal radius anatomy,^[1,4,8,15] rotational malalignment due to distal radius or shaft fractures,^[7,9,16] anatomic and kinematic studies of the carpal region,^[5,6,10] and DRUJ anatomy.^[5,11,12,17-19] Several anatomical locations have been used as principal axis of the distal radius in the past, including, the central axis,^[4,7-9,11,12,16] volar cortical axis at metaphyseal level,^[5,8,9] and sigmoid notch axis.^[5]

In the current study, a series of angular measurements based on axial CT images provided improved data for evaluating radiographic anatomy of the wrist. The main finding of the study is that there is considerable variability in the orientation among the four principal axes. In this study, the volar cortical and medial cortical axes are more consistent with the relatively fixed carpal unit than with the other principal axes.^[20]

Axial morphology of the volar surface of the distal radius has been examined in several studies.^[8,9,15] Based on CT scans of normal forearms, Oura et al.^[8] measured the angular difference between the central axis and each of volar cortical axes at 2-mm intervals from the joint. The entire

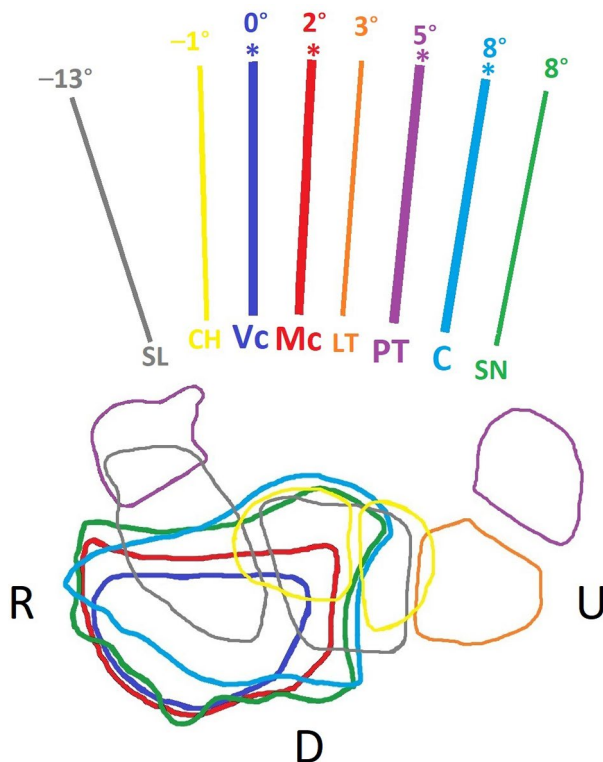


FIGURE 2. Combined representation of all axes and corresponding layers.

SL: Scapholunate axis; CH: Capitolunate axis; Vc: Volar cortical axis; Mc: Medial cortical axis; LT: Lunotriquetral axis; PT: Pisotrapezial axis; C: Central axis; SN: Sigmoid notch axis; R: Radial; D: Dorsal; U: Ulnar; * Principal reference axes.

volar cortex of the distal third of the radius presents a gradual external rotational angle from proximal to distal (from 14° to -2°) relative to the central axis. Recently, Daneshvar et al.^[9] performed a similar study and found a mean of 3° rotational difference between such principal radial axes, at the level of 15 mm proximal to the joint. However, the difference in our series was 8°. The discrepancy can be attributed to the fact that the aforementioned study used the reconstructed three-dimensional images of the cadaveric arms from older subjects. Moreover, the volar cortex appears in three different shapes on axial CT images: concave at the epiphyseal level,^[8,15] straight at metaphyseal level (particularly at 15 mm from the joint), and convex at the metaphyseal-diaphyseal level. Therefore, we preferred only the section 15 mm proximal from the joint.

The pisotrapezial and medial cortical axes are novel principal axes defined for this study. The pisotrapezial axis represents the subcutaneous bony prominences of both pisiform and trapezium contacted with the table/cassette while positioning of the wrist for posteroanterior X-ray. Its orientation remains between the medial cortical and the central axes (Figure 2). During posteroanterior positioning of the wrist, a firm contact of these volar subcutaneous bones with the cassette may provide a standardized image. Although this axis is located at the carpal level, it can be used as a principal axis for axial measurements in the radiocarpal region. The medial cortical axis is the closest principal axis to the volar cortical axis with a mean of 2°.

The sigmoid notch version angle is a fundamental axial parameter of the distal radius,^[5,11,12,17-19] This angle was used as a reference for kinematic studies of the DRUJ^[5] and associated with some clinical conditions including triangular fibrocartilage tear^[19] and DRUJ instability.^[11,19] Jung et al.^[19] found an association between the DRUJ instability and the flat-face type of sigmoid notch described by Tolat et al.^[21] A flat-faced sigmoid notch inherently has a lower version angle,^[19] and can be reconstructed with osteoplasty in case of instability.^[22] Our study provided reliable measurement values for the sigmoid notch version angle with a mean of 8° relative to the volar cortical axis, 6° with the medial cortical axis, 1° with central axis, and 4° with the pisotrapezial axis. We favored 8° of measurement (range, -2° to 18°), as the volar cortical axis is the most consistent one among the four principal axes. Overall, the sigmoid notch rotation angle tends to face dorsally (retroverted), but only one case had an anteverted

angle with -2°. Normative values of the sigmoid notch version angle have also been reported in a number of studies.^[5,11,12,17-19] Results of other studies are heterogeneous possibly, due to nonuniform measurement techniques. To illustrate, some^[17-19] have measured the sigmoid notch version angle with reference to the dorsal half of the sigmoid notch itself as the principal reference axis and obtained mean values of 9°, 10°, and 13°. This reference axis is non-linear and non-anatomical in our opinion and, therefore, we ignore their normative values.^[17-19] Two studies have also reported the sigmoid notch version angle relative to the central axis: Bade et al.^[12] with a mean of 6° (range 0°-19°) and Daneshvar et al.^[11] with a mean of -3° (anteverted) (range, -17° to 7°). However, using the same principal axis, our mean sigmoid notch version angle with a mean of 1° was slightly less than that of the former,^[12] greater than that of the latter.^[11] The discrepancy may be because the former study performed the measurements photographically on the cadaveric radiocarpal joint surfaces,^[12] and the latter performed digital measurement on three-dimensional CT images of cadaveric arms of elderly subjects.^[11] Finally, Gupta et al.^[5] measured the sigmoid notch version angle with a mean of 7° (range -16 to +31) relative to the volar cortical axis, which is similar to our result (mean: 8°) with the same axis.

The scapholunate joint exhibits a considerable external rotation in axial plane^[5] that may create overlapping of the adjacent articular surfaces of the scaphoid and lunate evident on routine posteroanterior X-ray and, therefore, a difficulty for detecting the widened scapholunate gap on posteroanterior radiographs can be experienced in case of a mild degree of scapholunate dissociation.^[13,23,24] To eliminate this normal rotation of the scapholunate joint, elevation of the ulnar border of the hand^[23,24] by 20° or tube angulation from the ulnar side toward the radius^[13] by 10° were suggested in two studies. Our study also provided reliable data for scapholunate joint rotation angle. The scapholunate joint formed a mean of -13° externally rotated angle with the volar cortical axis and -18° with the pisotrapezial axis. Kindynis et al.^[13] measured the scapholunate joint rotation with a mean of -13° with respect to the table, which is comparable to our values.

Nevertheless, there are several limitations to this study. First, it is a retrospective, cross-sectional study. Second, due to our relatively small sample size, we were unable to deem our measured values to be representative of a population and identify

ethnic variations. The final limitation is the lack of information on the intraobserver repeatability.

In conclusion, these axial descriptions represent consistent geometries between radial and carpal regions and provide a tool for understanding the comparative anatomy between them. A better understanding of normal axial anatomy of the wrist may enhance our ability to diagnose and treat wrist conditions such as DRUJ instability, scapholunate dissociation, and rotational malunions. These standardized axial measurements may be used in future studies on the distal radius, ulna, and carpal region.

Ethics Committee Approval: The study protocol was approved by the Ethical Committee for Clinical Research, Adana City Training and Research Hospital (date: 30.05.2022, no: 1954). The study was conducted in accordance with the principles of the Declaration of Helsinki.

Patient Consent for Publication: A written informed consent was obtained from each patient.

Data Sharing Statement: The data that support the findings of this study are available from the corresponding author upon reasonable request.

Author Contributions: Idea/concept: A.A., M.Y.H.; Design: A.A., M.Y.H.; Control/supervision: F.S.; Data collection and/or processing: B.Ö., M.Y.H.; Analysis and/or interpretation: A.A., B.Ö.; Literature review: A.A., M.Y.H.; Writing the article: A.A.; Critical review: F.S.; Materials: B.Ö., M.Y.H.; Gaining ethical approval: M.B., F.S.

Conflict of Interest: The authors declared no conflicts of interest with respect to the authorship and/or publication of this article.

Funding: The authors received no financial support for the research and/or authorship of this article.

REFERENCES

- Lee RK, Griffith JF, Ng AW, Wong CW. Imaging of radial wrist pain. I. Imaging modalities and anatomy. *Skeletal Radiol* 2014;43:713-24. doi: 10.1007/s00256-014-1840-7.
- Gürsan O, Açıkan AE, Asma A, Hapa O. Labral tears with axial plane disorders. *Jt Dis Relat Surg* 2020;31:109-14. doi: 10.5606/ehc.2020.70193.
- Günay C, Özçelik A. Is Stage 2 idiopathic osteonecrosis of the hip joint associated with version angles on imaging methods? *Jt Dis Relat Surg* 2021;32:611-6. doi: 10.52312/jdrs.2021.273.
- Bergsma M, Doornberg JN, Borghorst A, Kernkamp WA, Jaarsma RL, Bain GI. The watershed line of the distal radius: Cadaveric and imaging study of anatomical landmarks. *J Wrist Surg* 2020;9:44-51. doi: 10.1055/s-0039-1698452.
- Gupta A, Al Moosawi NM, Agarwal RP. In vivo CT study of carpal axial alignment. *Surg Radiol Anat* 2003;25:455-61. doi: 10.1007/s00276-003-0169-z.
- Camus EJ, Millot F, Larivière J, Raoult S, Raimate M. Kinematics of the wrist using 2D and 3D analysis: Biomechanical and clinical deductions. *Surg Radiol Anat* 2004;26:399-410. doi: 10.1007/s00276-004-0260-0.
- Filer J, Smith A, Giddins G. Assessing distal radius malrotation following fracture using computed tomography. *J Orthop Surg (Hong Kong)* 2019;27:2309499019862872. doi: 10.1177/2309499019862872.
- Oura K, Oka K, Kawanishi Y, Sugamoto K, Yoshikawa H, Murase T. Volar morphology of the distal radius in axial planes: A quantitative analysis. *J Orthop Res* 2015;33:496-503. doi: 10.1002/jor.22780.
- Daneshvar P, Willing R, Lapner M, Pahuta MA, King GJW. Rotational anatomy of the radius and ulna: Surgical implications. *J Hand Surg Am* 2020;45:1082.e1-1082.e9. doi: 10.1016/j.jhssa.2020.04.018.
- de Roo MGA, Dobbe JGG, Peymani A, van der Made AD, Strackee SD, Streekstra GJ. Accuracy of manual and automatic placement of an anatomical coordinate system for the full or partial radius in 3D space. *Sci Rep* 2020;10:8114. doi: 10.1038/s41598-020-65060-7.
- Daneshvar P, Willing R, Pahuta M, Grewal R, King GJ. Osseous anatomy of the distal radioulnar joint: An assessment using 3-dimensional modeling and clinical implications. *J Hand Surg Am* 2016;41:1071-9. doi: 10.1016/j.jhssa.2016.08.012.
- Bade H, Koebeke J, Schlüter M. Morphology of the articular surfaces of the distal radio-ulnar joint. *Anat Rec* 1996;246:410-4. doi: 10.1002/(SICI)1097-0185(199611)246:3<410::AID-AR12>3.0.CO;2-R.
- Kindynis P, Resnick D, Kang HS, Haller J, Sartoris DJ. Demonstration of the scapholunate space with radiography. *Radiology* 1990;175:278-80. doi: 10.1148/radiology.175.1.2315496.
- Schernberg F. Roentgenographic examination of the wrist: A systematic study of the normal, lax and injured wrist. Part 1: The standard and positional views. *J Hand Surg Br* 1990;15:210-9. doi: 10.1016/0266-7681_90_90126-o.
- Kumar A, Passey J, Chouhan D, Saini M, Narang A. CT based characterization of volar surface of distal radius: Can an ideal volar plate for fixation of distal radial fractures be designed? *J Hand Surg Asian Pac Vol* 2021;26:77-83. doi: 10.1142/S2424835521500120.
- Van Riet RP, Van Glabbeek F, Neale PG, Bimmel R, Bortier H, Morrey BF, et al. Anatomical considerations of the radius. *Clin Anat* 2004;17:564-9. doi: 10.1002/ca.10256.
- Collins ED, Vossoughi F. A three-dimensional analysis of the sigmoid notch. *Orthop Rev (Pavia)* 2011;3:e17. doi: 10.4081/or.2011.e17.
- Shivdas S, Hashim MS, Ahmad TS. A three-dimensional virtual morphometry study of the sigmoid notch of the distal radius. *J Orthop Surg (Hong Kong)* 2018;26:2309499018802504. doi: 10.1177/2309499018802504.
- Jung HS, Park MJ, Won YS, Lee GY, Kim S, Lee JS. The correlation between shape of the sigmoid notch of the distal radius and the risk of triangular fibrocartilage complex foveal tear. *Bone Joint J* 2020;102-B:749-54. doi: 10.1302/0301-620X.102B6.BJJ-2019-1284.R1.
- Atik OŞ. Which articles do the editors prefer to publish? *Jt Dis Relat Surg* 2022;33:1-2. doi: 10.52312/jdrs.2022.57903.
- Tolat AR, Stanley JK, Trail IA. A cadaveric study of the anatomy and stability of the distal radioulnar joint in the coronal and transverse planes. *J Hand Surg Br* 1996;21:587-94. doi: 10.1016/s0266-7681(96)80136-7.
- Kim BS, Song HS, Jung KH, Kim HT. Distal radioulnar joint volar instability after ligament reconstruction failure treated with sigmoid notch osteotomy. *Orthopedics* 2012;35:e984-7. doi: 10.3928/01477447-20120525-49.
- Moneim MS. The tangential posteroanterior radiograph to demonstrate scapholunate dissociation. *J Bone Joint Surg [Am]* 1981;63:1324-6.
- Imada AO, Welch K, Mlady G, Moneim MSA. The tangential view described by Moneim to demonstrate scapholunate dissociation: An update. *Eur J Orthop Surg Traumatol* 2022. doi: 10.1007/s00590-022-03391-z.